

# Phototoxic aptamers selectively enter and kill epithelial cancer cells

Cátia S. M. Ferreira<sup>1</sup>, Melissa C. Cheung<sup>1</sup>, Sotiris Missailidis<sup>2</sup>, Stuart Bisland<sup>1</sup> and Jean Gariépy<sup>1,\*</sup>

<sup>1</sup>Ontario Cancer Institute, University Health Network, Ontario, Canada M5G 2M9 and <sup>2</sup>The Open University, Walton Hall, Milton Keynes, MK7 6AA, UK

Received August 15, 2008; Revised November 13, 2008; Accepted November 14, 2008

## ABSTRACT

**The majority of cancers arise from malignant epithelial cells. We report the design of synthetic oligonucleotides (aptamers) that are only internalized by epithelial cancer cells and can be precisely activated by light to kill such cells. Specifically, phototoxic DNA aptamers were selected to bind to unique short O-glycan-peptide signatures on the surface of breast, colon, lung, ovarian and pancreatic cancer cells. These surface antigens are not present on normal epithelial cells but are internalized and routed through endosomal and Golgi compartments by cancer cells, thus providing a focused mechanism for their intracellular delivery. When modified at their 5' end with the photodynamic therapy agent chlorin e<sub>6</sub> and delivered to epithelial cancer cells, these aptamers exhibited a remarkable enhancement (>500-fold increase) in toxicity upon light activation, compared to the drug alone and were not cytotoxic towards cell types lacking such O-glycan-peptide markers. Our findings suggest that these synthetic oligonucleotide aptamers can serve as delivery vehicles in precisely routing cytotoxic cargoes to and into epithelial cancer cells.**

## INTRODUCTION

Oligonucleotides cannot traverse cell membranes, a feature that restricts their therapeutic potential either as modulators of intracellular cell functions or as carriers of therapeutic agents. However, short, single-stranded RNA or DNA oligonucleotides known as aptamers (1,2) have been shown to adopt distinct 3D structures complementary to a given molecular target. They are derived from an initial combinatorial pool of random oligonucleotide sequences using an *in vitro* selection approach termed SELEX (Systematic Evolution of Ligands by Exponential Enrichment (3,4)). By judiciously selecting cell surface

structures as targets for aptamer searches, one can derive aptamers that can specifically recognize internalized surface markers (portals) and thus be imported into cells. A case in point is the use of RNA aptamers recognizing the human prostate antigen PSMA, to deliver siRNA molecules into such cells (5). Membrane-associated glycoforms of mucin glycoproteins represent an important class of tumor surface markers that are uniquely and abundantly expressed on a broad range of epithelial cancer cells (breast, ovary, colon, pancreas, lung and prostate) (6,7). These markers are also rapidly recycled through intracellular compartments (endosomes, Golgi) (8–11), and thus can serve as entry portals for aptamers. Mucins typically harbour variable numbers of peptide tandem repeats (VNTR) rich in serine, threonine and proline residues (12) where serines and threonines are post-translationally modified with O-linked oligosaccharides (O-glycans). Carbohydrate chains account for more than 50% of their mass (12). The aberrant glycosylation of mucins has been shown to promote a metastatic phenotype (13–15). Shortened carbohydrate chains and peptide epitopes are revealed as a consequence of incomplete O-glycosylation events occurring in these cells. Monoclonal antibodies raised against tumour-associated forms of MUC1 commonly recognize part of the mucin exposed peptide backbone or the Tn (GalNAc) and T (Galβ1-3GalNAc) antigens O-linked to the peptide tandem repeat (16). We have recently generated a peptide corresponding to five consecutive mucin MUC1 tandem repeats (MUC1-5TR) and biosynthetically introduced GalNAc sugars (MUC1-5TR-GalNAc; Tn antigens) within its structure (17) with a view to deriving short, single-strand DNA aptamers displaying a more focused specificity for these tumour antigens than monoclonal antibodies. We now report that these 25-base long synthetic DNA aptamers are efficiently internalized by epithelial cancer cells and can be used as delivery vehicles to specifically route pro-drug cargoes such as photodynamic therapy (PDT) agents into such cells to kill them.

\*To whom correspondence should be addressed. Tel: +1 416 946 2967; Fax: +1 416 946 6529; Email: gariépy@uhnres.utoronto.ca

## MATERIALS AND METHODS

### Reagents for SELEX screens

We initially engineered mimics of known mucin MUC1 determinants (17) on cancer cells namely a recombinant deglycosylated peptide representing five MUC1 tandem repeats (MUC1-5TR) and its *O*-glycosylated form containing 15 GalNAc sugars (Tn antigens, MUC1-5TR-GalNAc) to serve as targets in selecting DNA aptamers. Briefly, a synthetic gene coding for five copies of the MUC1 tandem repeat and a N-terminal hexahistidine metal affinity tag (MUC1-5TR) was inserted into the pET-15b expression vector (Novagen, Madison, WI). The resulting construct was used to transform competent *Escherichia coli* BL21 (DE3) cells (Novagen) and the expression of MUC1-5TR induced with isopropyl  $\beta$ -D-thiogalactopyranoside (IPTG). MUC1-5TR was purified by nickel affinity chromatography under denaturing conditions. The sequence of the purified MUC1-5TR was confirmed by mass spectrometry and the peptide was stored at  $-20^{\circ}\text{C}$  until use. MUC1-5TR was enzymatically modified with up to 15 GalNAc sugars (Tn antigen) using a recombinant secreted form of the human ppGalNAc-T1 expressed in *Pichia pastoris* (17). Unglycosylated MUC1-5TR or its Tn-labelled form (3 mg) were separately immobilized onto 1 mm HiTrap Chelating HP columns (GE Healthcare, Baie d'Urfé, Québec). The target loaded matrices were subsequently used for aptamer selection. In the case of *N*-acetylgalactosamine being used as a target, plates covalently modified with this sugar were purchased from EMD Biosciences (Mississauga, Ontario). Briefly, GalNAc determinants were directly coupled using an amide linkage to wells of a 96-well polystyrene plate via a 16–18 atom flexible spacer, providing a homogeneous presentation of the target to putative DNA aptamers emerging as strong ligands. Plates were kept at  $-20^{\circ}\text{C}$  for the duration of the experiment, except during ssDNA library incubation times. *In vitro* selection strategies based on SELEX approach were developed to identify aptamers that bind to all three targets under physiological conditions (150 mM NaCl, 5 mM MgCl<sub>2</sub>, pH 7.4, 37°C. (Figure 1a, Table 1). The selection of MUC1 DNA aptamers is described in Supplementary Data section 1 and in ref. (18). Selected aptamer pools were amplified by asymmetric PCR (aPCR) using an excess of forward primer (1000 $\times$ ) and limiting the amount of reverse primer (1 $\times$ ) to favour the production of sense (5' to 3') single-stranded DNA products (DNA aptamers) (19).

All subsequent oligonucleotides were purchased from Midland Certified Reagent Co (Midland, Texas, USA) either as unmodified aptamers or labelled at their 5' amino end with biotin, chlorin *e*<sub>6</sub> or Rhodamine101.

### Electrophoretic mobility shift assays (EMSA)

The association of DNA aptamers recognizing MUC1 peptide constructs with their respective target was confirmed by a shift in their electrophoretic mobility in a 6% polyacrylamide pre-cast DNA retardation gel (Invitrogen, Burlington, Canada) upon complexation

with their target. Qualitative EMSA was performed using a binding reaction mixture (20  $\mu$ l) composed of 100 mM NaCl, 5 mM MgCl<sub>2</sub>, 100 mM KCl, 1 mM dithiothreitol, 5% glycerol, a protein target (5  $\mu$ l, 1 mg/ml) and a <sup>32</sup>P-labelled DNA aptamer. The mixture was incubated for 30 min at room temperature and electrophoretically resolved at a constant voltage of 150 V for 2 h at room temperature. The running buffer was 1/2  $\times$  TBE (0.045 M Tris borate, pH 8, 1 mM EDTA). The gel was subsequently dried and exposed to film.

### Surface plasmon resonance (SPR) measurements

All SPR-binding measurements were recorded on a BIAcore 3000 instrument using nickel NTA sensor chips (CM5 chip; GE Healthcare, Baie d'Urfé, Québec). The MUC1 peptide antigens carry a hexa histidine tag and were directly immobilized onto NTA chips by dissolving each antigen in 10 mM sodium acetate (pH 5.2) and injecting them onto a chip at a concentration of 500  $\mu$ g/ml. The chips were equilibrated in a binding buffer (100 mM NaCl, 5 mM MgCl<sub>2</sub> (pH 7.4) that also served as the running buffer. The flow rate was 5  $\mu$ l/min. Calculations of kinetic parameters from SPR measurements are presented in Supplementary Data section 2.

The DNA aptamers were refolded in the binding buffer for the dose-dependent binding assays and injected over the flow cells. The surfaces were regenerated between injections using two 5  $\mu$ l injections of 10 mM NaOH, followed by a 10-min wash step with the running buffer. The association and dissociation rate constants for aptamer-peptide and aptamer-sugar complexes were determined using a non-linear regression analysis for the initial parts of association and dissociation phases of the sensograms. (7.5 Origin Pro software; MicroCal).

### Flow cytometry and internalization studies

Rhodamine-labelled aptamers (200 pmol) were incubated with 10<sup>5</sup> cells of either MCF-7, T47D, PANC-1 or CHO cells at 37°C for 30 min to determine the level of MUC1 expression on their surface. Cells were trypsinized, washed three times with PBS and counted using a hemocytometer. The cells were resuspended in 500  $\mu$ l of PBS and 4% FBS and incubated with either 200 pmol of a rhodamine-labelled aptamer or with the mAb *OncM27* (20) for 30 min at 37°C. Cells were subsequently washed three times with PBS and the antibody-stained cells were further incubated with 1:1500 dilution of FITC-labelled anti-mouse antibody (BD Biosciences, Franklin Lakes, NJ) in PBS. After a 30 min incubation period, cells were washed three times with PBS and analysed by flow cytometry (FACScan; BD Biosciences, Franklin Lakes, NJ). Internalization studies were carried out as described above, with the added modifications that all aptamers and mAb *OncM27* were incubated at 37°C or at 4°C (on ice) for the period of time ranging from 30 min to 6 h.

### Confocal microscopy

MCF-7, T47D, PANC-1 or CHO cells were grown in duplicate wells of four-well chambered coverglass tissue culture microscopy plates (NUNC). Cell medium was

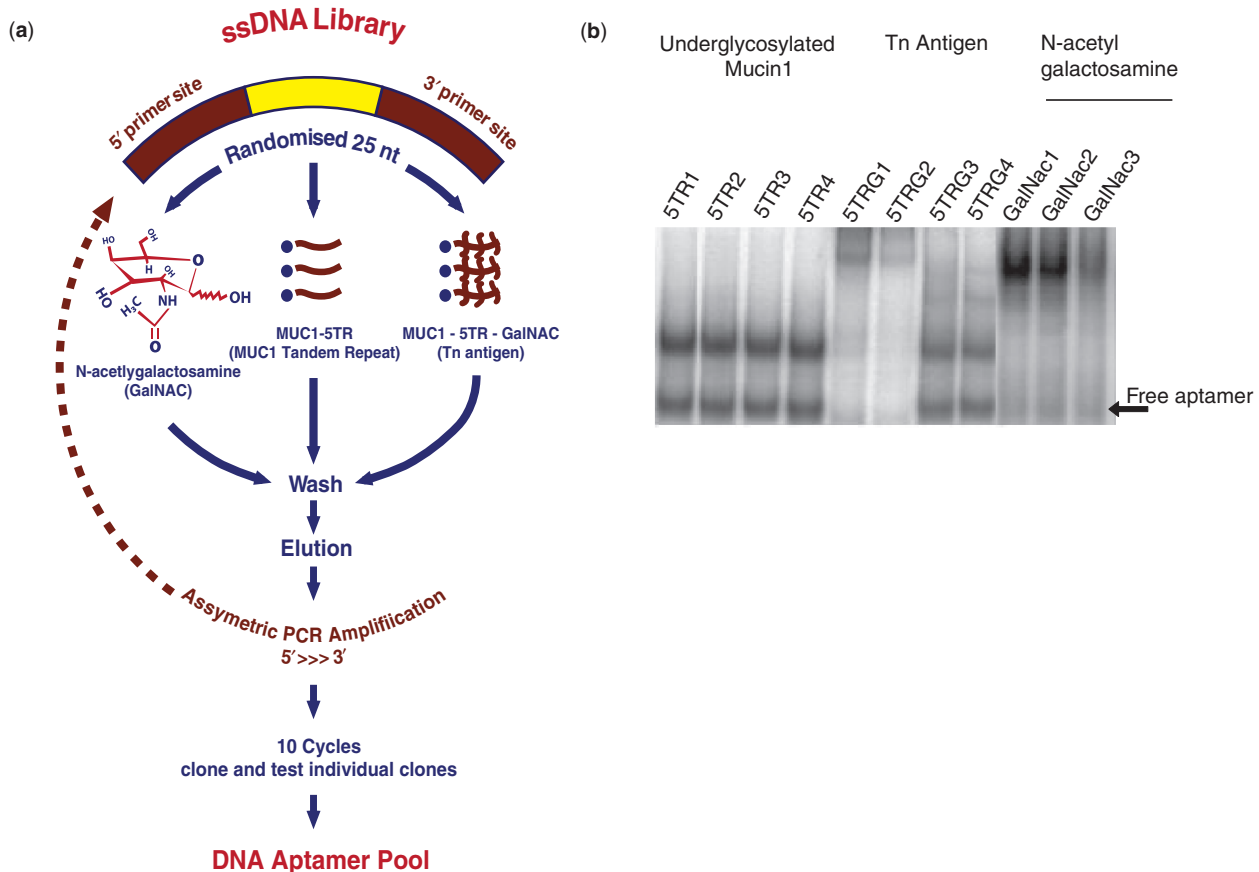


**Figure 1.** (a) Schematic representation of the selection process leading to the discovery of epithelial tumour-specific DNA aptamers. Single-strand DNA oligonucleotides were derived using the SELEX (systematic evolution of ligands by exponential enrichment) approach (4). Specifically, a pool of ssDNAs displaying a 25 nt random region was incubated with either His-tagged MUC1-5TR peptide or its GalNAc-modified variant (Tn antigen) bound to nickel-NTA beads or with *N*-acetylgalactosamine immobilized in wells of a 96-well plate. Bound oligonucleotides were recovered using a high salt step, desalted and amplified by asymmetric PCR before a new cycle of selection. After 10 rounds of selection, each DNA aptamer pool was cloned and sequenced. Individual aptamers were synthesized and further analysed to assess their specificity. (b) Binding specificity of DNA aptamers to their respective target. The association of 11 distinct DNA aptamers (Table 1) recognizing MUC1 peptide constructs (MUC1-5TR, Tn antigen) as well as the carbohydrate *N*-acetylgalactosamine (GalNAc) with their respective target was further confirmed using an electrophoretic mobility shift assay (EMSA). Aptamers were incubated with their target for 30 min and resolved on a 6% polyacrylamide DNA retardation gel. DNA-peptide complexes were observed when aptamers 5TR1, 5TR2, 5TR3 and 5TR4 were mixed with their target namely unglycosylated MUC1-5TR. Similarly, complexes were observed when aptamers 5TRG1, 5TRG2, 5TRG3, 5TRG4, GalNAc1, GalNAc2 and GalNAc3 were added to the peptide MUC1-5TR-GalNAc (Tn antigen). Individual DNA aptamers derived from different glycosylated targets (Tn antigen versus GalNAc alone) displayed distinct band shifts with the MUC1-5TR-GalNAc peptide (Tn antigen). The higher mass species observed for all GalNAc-specific aptamers bound to glycosylated MUC1 (MUC1-5TR-GalNAc) reflect the higher molar ratio of bound aptamers (GalNAc1, GalNAc2 and GalNAc3) recognizing up to 15 GalNAc groups per MUC1-5TR-GalNAc peptide (17) while aptamers recognizing features from both peptide and sugar components (5TRG1, 5TRG2, 5TRG3, 5TRG4) yielded distinct band migration profiles.

removed from each well and cells were further washed three times with PBS. Rhodamine-labelled aptamers or the mAb OncM27 were dissolved in PBS and added to the wells at concentrations ranging from 0.05 pmol/ $\mu$ l to 1 pmol/ $\mu$ l. Plates were incubated for 30 min at 37°C. Wells were washed three times with PBS and treated with 2  $\mu$ l per 1000  $\mu$ l of a 2% (w/v) BSA solution prepared in PBS. In the case of the mAb OncM27, a second labelling step was necessary with a FITC-labelled anti-mouse antibody (Pharmingen, Becton Dickinson) for 30 min at 37°C. Cells were washed three times and kept in 20 mM Hepes buffer prior to microscopy. Either 100  $\mu$ l of PBS (control) or 100  $\mu$ l of a 0.25 pmol/ $\mu$ l solution of a fluorescently labelled aptamer in PBS were dispensed in each well. The DNA aptamers were allowed to complex with MUC1 targets

present on the surface of cells for 30 min. Individual wells were washed three times with 1 ml of PBS. Adherent cells in wells were visualized using a Two-Photon Zeiss LSM 510 META NLO microscope, HeNe Laser—(543 nm) HeNe Laser—(633 nm), C-Apo 40 $\times$ /1.2 NA lens, at 40  $\times$  1.6  $\times$  10 magnification, and analysed with LSM150 image browser software. Phase-contrast and confocal images (2  $\mu$ m thickness) of viable cells were taken after the 30 min incubation period.

#### Photodynamic treatment

The PDT agent chlorin  $e_6$  was introduced post-synthesis at the 5' amino group of DNA aptamers. Briefly, a single carboxylic acid of chlorin  $e_6$  was coupled with EDC

**Table 1.** List of nucleotide sequences defining the specificity of each DNA aptamer

5' > GGGAGACAAGAATAAACGCTCAA <3' (Forward primer)		
5' > GCCTGTTGTGAGCCTCCTGTCGAA <3' (Reverse primer) 5'		
5'GAGACAAGAATAAACGCTCAA-(N25)-TTCGACAGGAGGCTCACAACAGGC '3		
5TR1	GAAGTAAAAATGACAGAACACAACA	25nt
5TR2	GGCTATAGCACATGGGTAACGAC	25nt
5TR3	CAAACAATCAAACAGCAGTGGGGTG	25nt
5TR4	TACTGCATGCACACCCTCAACTA	25nt
5TRG1	GGGTTATATTACTCGGCCGGTGTA	25nt
5TRG2	GGCTATAGCACATGGGTAACGAC	25nt
5TRG3	GGCGTACGGTAGGCGGGTCAACTG	25nt
5TRG4	GCTGGGTAATAGATGATTCCCGGC	25nt
GalNac1	AGACTTAGGTGGATGTAGGATCCTT	25nt
GalNac2	CTCCGATCCACTAGTAACGGCCGCC	25nt
GalNac3	AAGGGATGACAGGATACGCCAAGCT	25nt

(0.1 M in DMF) to the amino group of aptamers (dissolved in potassium phosphate, pH 7.0) using a 1:3:3 molar ratio of aptamer to chlorin  $e_6$  and EDC. The coupling mixtures were left to react overnight at 60°C in the dark. The conjugates were then loaded on a C<sub>18</sub> column equilibrated in 0.1 M sodium acetate, pH 7.0 and eluted with a gradient of the same buffer going from 0% to 40% AcN. Aliquots of  $5 \times 10^3$  cells of either human cancer cells (T47D, MCF-7, PANC-1, BxPC3, A549, MGH13, OVCAR-3, HT-29, U87MG), CHO cells or normal human primary mammary epithelial cells (HMEC) (Clonetics; Lonza, Basel, Switzerland) suspended in 200  $\mu$ l growth medium were seeded into wells of blackened 96-well plates with clear bottoms (Corning Costar Corp., Cambridge, MA) and cultured for 6 h at 37°C in the presence of 5% CO<sub>2</sub>. Cells were treated with PBS or increasing concentrations of either chlorin  $e_6$  or chlorin  $e_6$ -aptamers followed by light activation treatments. Control samples were also prepared and kept from light. Wells were irradiated with 664 nm light from above using an optic fibre coupled to a dye laser source (Spectra Physics model 375B), applying a radiant exposure of 12 J/cm<sup>2</sup> at fluency rate of 20–30 mW/cm<sup>2</sup>. Once irradiated, cells were incubated with fresh growth medium for an additional 48 h at 37°C in the dark. Cell viability was assessed using a methyltetrazolium salt (MTT) colorimetric assay (21). Specifically, 24 h following aptamer or chlorin  $e_6$  treatment and light activation, cells were incubated with methyl-tetrazolyl tetrazolium (2 mg/ml) for 4 h at 37°C. The medium was then replaced with 100  $\mu$ l dimethylsulfoxide and the plates shaken for 5 min. Absorbance was read at the 570 nm and dose-response curves were plotted using GraphPad Prism software for experiments performed in triplicate.

#### Photoinduced oxidative burst

MCF-7 and T47D cells ( $2 \times 10^4$  cells) were seeded onto a Lab-Tek coverglass 2 chamber slide in 1 ml of growth medium containing 0.01  $\mu$ M chlorin  $e_6$ -aptamers and

incubated (37°C, 5% CO<sub>2</sub>) for 1 h in the dark and then washed with PBS (three times) under strictly subdued light conditions. Cells were exposed for 25 min at 37°C in medium containing 5  $\mu$ M of 5 (and 6)-chloromethyl-2',7'-dichlorodihydrofluorescein diacetate (CM-H<sub>2</sub> DFDA) Slides remained at room temperature in the dark until analysed by confocal microscopy. Single cells were visualized before and after light activation of chlorin  $e_6$  or chlorin  $e_6$  aptamers. Reactive oxygen species (ROS) signals were recorded using a scanning confocal imaging system (Argon-ion laser; 488/514.5 nm; MRC 600, Bio-Rad Laboratories Ltd, Ont., Canada). Signals were viewed through a 63 $\times$ /0.55 Nikon water-immersible objective lens. Chlorin  $e_6$  was activated using a helium cadmium (HeCd) laser (omNichrome series 56). The fluorescence signal from CM-H<sub>2</sub> DFDA was simultaneously recorded using a green filter, allowing for a direct intracellular visualization of fluorescent signals over a 10 s period.

## RESULTS

### Aptamer selection and characterization

We recently engineered mimics of known mucin MUC1 determinants on cancer cells namely a recombinant deglycosylated peptide representing five MUC1 tandem repeats (MUC1-5TR) and its *O*-glycosylated form containing 15 GalNAc sugars (Tn antigens; MUC1-5TR-GalNAc) (17) to serve as targets in selecting DNA aptamers (Figure 1). In addition, an immobilized form of *N*-acetylgalactosamine (GalNAc) was used as a target to define DNA aptamers that only recognize the carbohydrate component of MUC1-5TR-GalNAc. Eleven aptamers displaying nanomolar-binding constants for their respective targets are presented in Tables 1 and 2. A comparison of calculated  $K_d$  values for all aptamers binding to MUC1 peptides lacking or not GalNAc sugars (Table S1) suggests that they can readily differentiate peptide targets harbouring or not GalNAc residues.

**Table 2.** Kinetic parameters and calculated  $K_d$  values for DNA aptamers

Aptamer	SELEX target	$k_a$ ( $M^{-1}s^{-1}$ ) <sup>a</sup>	$k_d$ ( $s^{-1}$ ) <sup>a</sup>	$K_d$ (nM)
5TR1	MUC1-5TR	$1.22 \times 10^7$	0.0026	21.0
5TR2	MUC1-5TR	$1.48 \times 10^7$	0.01268	85.2
5TR3	MUC1-5TR	$0.43 \times 10^7$	0.00358	83.0
5TR4	MUC1-5TR	$0.45 \times 10^7$	0.00311	69.0
5TRG1	Tn antigen	$1.33 \times 10^7$	0.00398	25.1
5TRG2	Tn antigen	$1.02 \times 10^7$	0.0186	18.6
5TRG3	Tn antigen	$0.92 \times 10^7$	0.00252	27.2
5TRG4	Tn antigen	$0.91 \times 10^7$	0.00314	34.4
GalNAc1	<i>N</i> -Acetylgalactosamine	$1.33 \times 10^7$	0.0801	59.8
GalNAc2	<i>N</i> -Acetylgalactosamine	$2.02 \times 10^7$	0.1199	58.3
GalNAc3	<i>N</i> -Acetylgalactosamine	$0.21 \times 10^7$	0.00098	47.3

<sup>a</sup> $\chi^2 > 0.981$ .**Selected aptamers bind specifically to cells expressing MUC1 glycoforms**

DNA aptamers displaying the highest affinity constant for their respective target, namely 5TR1, 5TRG2 and GalNAc3 (Table 2), were labelled at their 5' end with rhodamine and their binding to cells expressing MUC1 glycoforms analysed by flow cytometry and by two-photon confocal microscopy (Figure 2). The monoclonal antibody *OncoM27* (20) recognizes the peptide epitope TRP within the MUC1 tandem repeat (16) and was used to confirm the expression of MUC1 mucin on all cell lines tested (see Figure S1, Supplementary Data). The flow cytometric profiles presented in Figure 2, indicate that all three fluorescent aptamers as well as the mAb

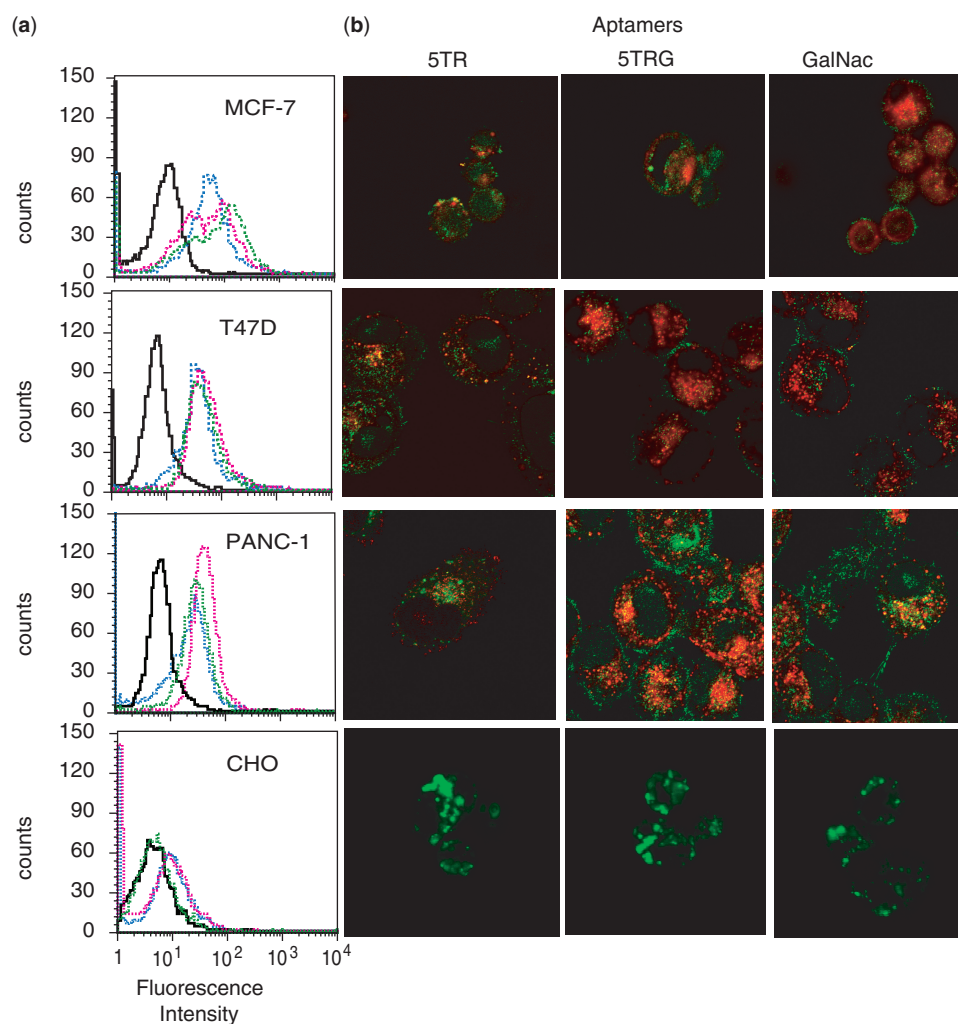


**Figure 2.** (a) Selective binding of DNA aptamers to tumour-specific MUC1 determinants on cancer cells. The cancer cell lines MCF-7 (MUC1<sup>+</sup> human breast cancer), T47D (MUC1<sup>+</sup> human breast cancer), PANC-1 (MUC1<sup>+</sup> human pancreatic cancer) as well as CHO cells (MUC1<sup>-</sup> Chinese hamster ovary; negative control) were stained with rhodamine-labelled DNA aptamers and analysed by flow cytometry. Cell-type specific binding was observed for aptamers 5TR1 (blue), 5TRG2 (pink) and GalNAc3 (green). The background autofluorescence of unstained cells (black line) is shown for each cell line. Cells were also stained with the mAb *OncoM27* (recognizes the mucin MUC1 tandem repeat; Supplementary Figure S1) to confirm the expression of MUC1 determinants on cancer cells. (b) Specific staining of MUC1 and Tn antigen tumour markers on cancer cells as monitored by confocal microscopy. MCF-7, T47D, PANC-1 and CHO (negative control) cells were stained with three representative rhodamine-labelled MUC1 aptamers (red), namely 5TR1 binding to the unglycosylated MUC1 tandem repeat core, 5TRG2 recognizing peptide-GalNAc (Tn antigen) determinants and the aptamer GalNAc3 staining terminal GalNAc groups. Confocal images of viable cells recorded at 37°C were taken 30 min post incubation. Composite images were created to reveal the routing of rhodamine-aptamers to endosomal and lysosomal compartments (Lysotracker-stained (green) organelles). As a control, cells were also stained with the mAb *OncoM27* (recognizes the mucin MUC1 tandem repeat; Figure S1) and confocal images recorded to confirm the internalization of MUC1 and Tn antigen markers.

*OncM27* (Figure S1) recognize their determinants on MUC1-expressing epithelial cancer cell lines [MCF-7 (human breast cancer), T47D (human breast cancer) and PANC-1 (human pancreatic cancer)], while the same probes fail to bind to CHO cells (MUC1<sup>-</sup> cells). The two-photon confocal images presented in Figure 2 further illustrate that the chosen aptamers are able to recognize either the MUC1 peptide backbone or GalNAc determinants associated with the mucin MUC1 tandem repeat. As expected, no cell staining was observed for MUC1<sup>-</sup> CHO cells.

#### Aptamers as selective delivery vehicles into epithelial cancer cells

The anionic character of oligonucleotides does not favour their spontaneous entry into cells. However,

epithelial cells recycle underglycosylated forms of mucin MUC1 from their surface to the *trans*-Golgi network to further modify their glycan structure. MUC1 has been shown to be recycled through endosomal/lysosomal and the *trans*-Golgi network from the apical surface several times, a process that is accompanied by further sialylation of the *O*-glycans (9–11,22). To determine if our aptamers could be transported into cells by virtue of their association with MUC1 targets, we measured the time-dependent cellular uptake of rhodamine-labelled aptamers 5TR1, 5TRG2 and GalNAc3 by flow cytometry at 4°C and 37°C as well as in the presence of monodansyl cadaverine, an inhibitor of coated pit formation and receptor-mediated endocytosis (Figure 3) (23–25). As predicted, the aptamers 5TR1, 5TRG2 and GalNAc3 were rapidly endocytosed by MUC1<sup>+</sup> cells at 37°C but not at 4°C or by

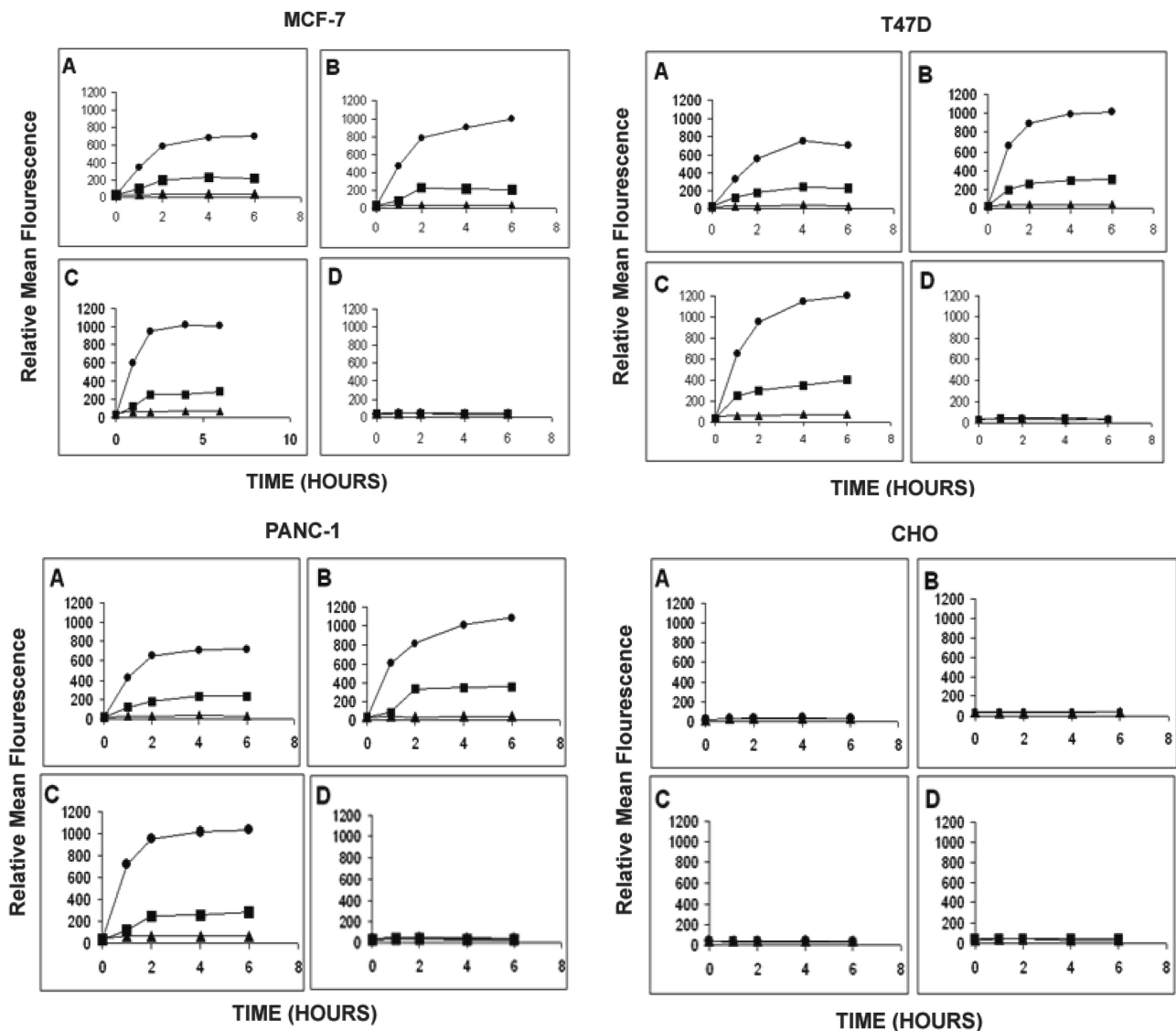


**Figure 3.** Time-dependent internalization of rhodamine-labelled aptamers into MCF-7, T47D, PANC-1 and CHO cells as measured by flow cytometry. Incubations were performed at 4°C (filled triangle), 37°C (filled circle) or in the presence of monodansyl cadaverine (filled square; 37°C) for up to 6 h. In all panels, curves represent the time-dependent changes in relative mean fluorescence intensities for cells exposed to 5TR1 aptamer (a), 5TRG2 aptamer (b), GalNAc3 aptamer (c), or an irrelevant 25 base-long DNA aptamer composed of GATC repeats (d). All data points represent the average relative mean fluorescence intensities derived from experiments performed in triplicate.

MUC1<sup>-</sup> cells (Figure 3). Their cellular uptake was significantly inhibited by monodansylcadaverine suggesting that their entry into MUC1<sup>+</sup> cells occurred by receptor-mediated endocytosis (Figure 3). A control irrelevant aptamer did not enter either MUC1<sup>+</sup> or MUC1<sup>-</sup> cells (Figure 3d). Thus, the evaluated DNA aptamers remained membrane-impermeant unless they were able to associate with an internalized surface marker. In terms of cellular localization, confocal microscopy images indicate that internalized DNA aptamers migrate through endosomal, lysosomal as well as through Golgi compartments and potentially to the cytosol of epithelial cancer cells but not to the ER lumen or nucleus of MUC1<sup>+</sup> cells (Figures 2 and 4).

#### Light-activated aptamers selectively kill epithelial cancer cells

PDT drugs are activated by light to produce cytotoxic singlet oxygen species. Their effectiveness as therapeutic agents is dependent on their cellular delivery. Since, aptamers 5TR1, 5TRG2 and GalNAc3 are selectively delivered into epithelial cancer cells, we introduced at their 5' end, the heme-like PDT agent chlorin *e*<sub>6</sub> (Ce6). Our aim was to demonstrate that, by virtue of their guided cellular targeting and intracellular routing, PDT-aptamers can target and kill MUC1 presenting cancer cells at much lower doses of chlorin *e*<sub>6</sub> than the free drug itself. As presented in Figure 5, chlorin *e*<sub>6</sub>-aptamers directed at eight MUC1<sup>+</sup> epithelial cancer cell lines (T47D, MCF-7, PANC-1, BxPC3, A549, MGH13, OVCAR-3, HT-29) were >500 times more toxic (on a molar basis) upon

light activation than the free drug chlorin *e*<sub>6</sub>. More importantly, these same aptamers were not toxic towards MUC<sup>-</sup> cells (CHO cells, U87MG cells) or MUC1<sup>+</sup> normal human primary mammary epithelial cells displaying fully glycosylated MUC1 mucin (Figure 5). Finally, DNA aptamers lacking the chlorin *e*<sub>6</sub> group or a chlorin *e*<sub>6</sub>-aptamer harbouring an irrelevant nucleotide sequence were not able to kill either MUC1<sup>+</sup> or MUC1<sup>-</sup> cells (Figure 5). The dramatic enhancement in cellular toxicity with chlorin *e*<sub>6</sub>-aptamers upon light treatment can be rationalized by the production and rapid cellular re-distribution of toxic singlet oxygen species throughout cancer cells (oxidative burst). This phenomenon was visualized in cells as the result of capturing the emission of light by chloromethyl-2',7'-dichlorodihydrofluorescein diacetate/AcrO upon reaction with the generated <sup>1</sup>O<sub>2</sub> species (Figure 6a).

#### DISCUSSION

The directed delivery of membrane-impermeant therapeutic oligonucleotides into diseased cells represents an essential criterion for improving their safety, cost and efficacy in *in vivo* settings. These important parameters must be addressed in devising targeted cancer therapies that can home on cancer cells while sparing normal tissues. We present evidence that internalized surface markers such as underglycosylated mucin MUC1 antigens can act as highly selective portals in importing oligonucleotides such as DNA aptamers into a broad range of epithelial cancer cells (breast, ovary, prostate, pancreas, colon and lung). When aptamers directed at the MUC1

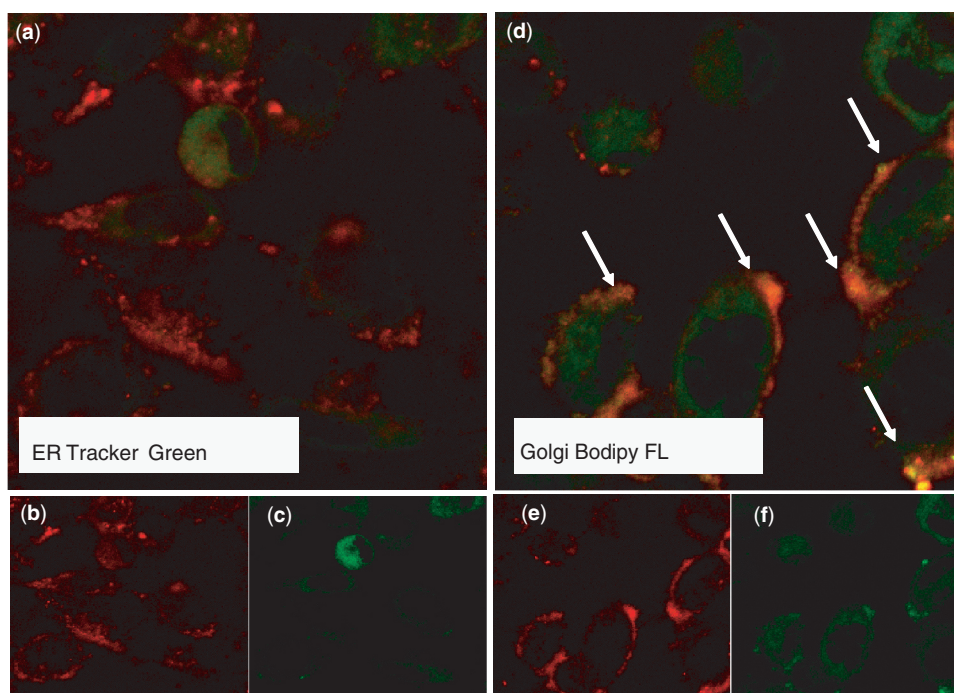


**Figure 4.** The DNA aptamer 5TRG2 is routed through Golgi compartments but not the ER lumen or nucleus of MUC1<sup>+</sup> cells. Viable T47D cells were stained with both ER Tracker selective for endoplasmic reticulum (green; c) and Golgi Bodipy FL selective for the Golgi complex (green; f) dyes as well as with rhodamine-labelled aptamer 5TRG2 (red; b and e). Composite images (a and d) derived from two-photon confocal images suggest that the aptamer 5TRG2 only reaches Golgi compartments in T47D breast cancer cells (white arrows).

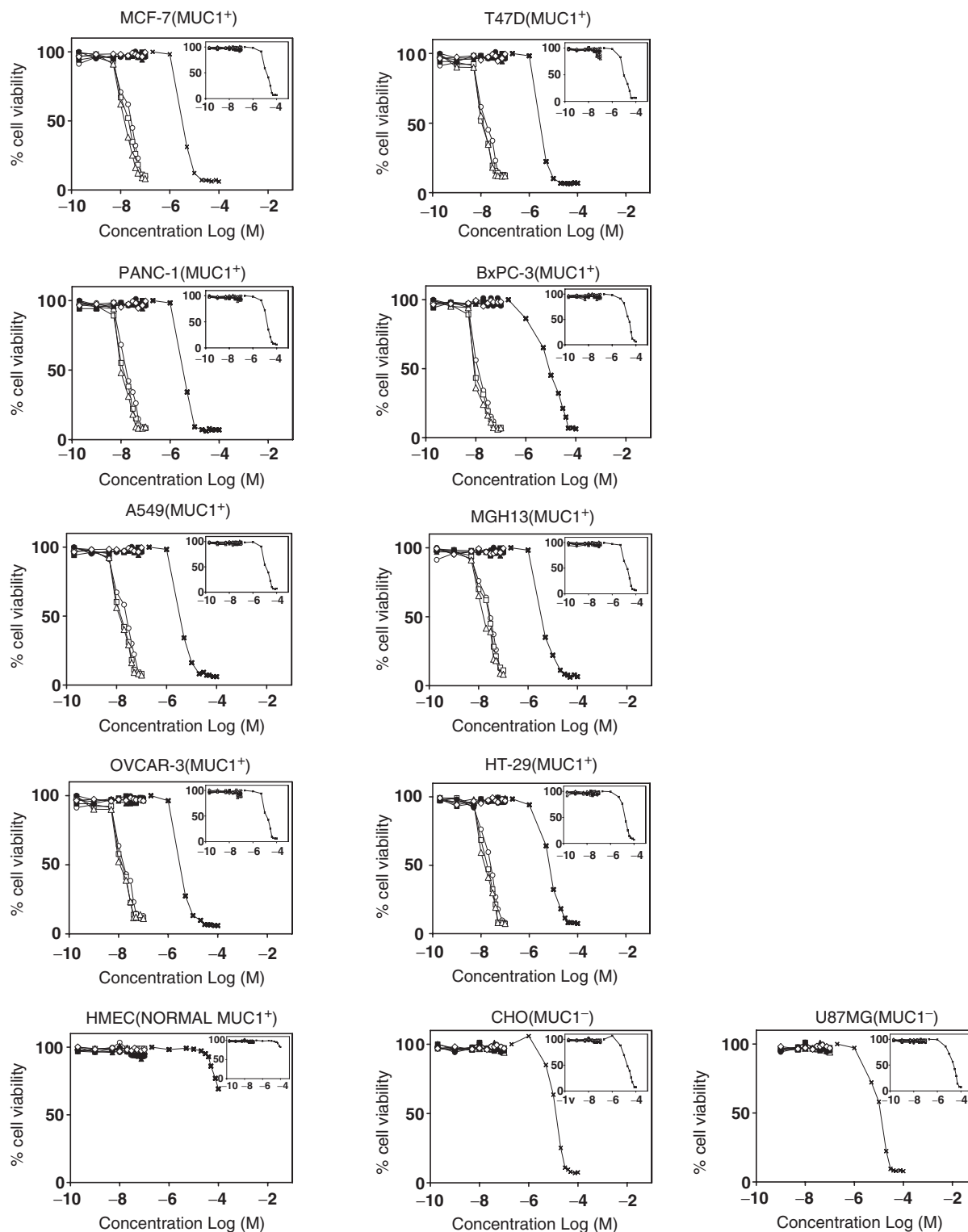


**Figure 5.** DNA aptamers labelled with the photodynamic agent chlorin  $e_6$  selectively kill epithelial cancer cells. Cell viability curves were constructed for eight MUC1<sup>+</sup> human cancer cells (human breast cancer cell lines T47D and MCF-7, human pancreatic cancer cell lines PANC-1 and BxPC3, human lung cancer cell lines A549 and MGH13, human ovarian cancer cell line OVCAR-3, colon cancer cell line HT-29), two MUC1<sup>-</sup> cell lines (Chinese Hamster Ovary cells [CHO], human malignant glioma cell line U87MG) as well as fully glycosylated MUC1<sup>+</sup> normal human mammary epithelial cells (HMEC). Cells were incubated in the presence of increasing concentrations of chlorin  $e_6$  alone (x), or either chlorin  $e_6$ -labelled Ce6-5TR1 aptamer (open square), Ce6-5TRG2 aptamer (open triangle), Ce6-GalNAc3 aptamer (open circle), unmodified 5TR1 aptamer (filled square), 5TRG2 aptamer (filled triangle), GalNAc3 aptamer (filled circle), or a Ce6-irrelevant aptamer (open diamond). Cell viability was determined for cells exposed (full graph) or not (captioned graph within each graph) to photoirradiation and reported as the percentage surviving cells measured in a MTT assay. The term concentration refers to the molar concentration of chlorin  $e_6$  either as a free drug or conjugated to aptamers. The irrelevant DNA aptamer used was a 25 base-long oligonucleotide composed of GATC repeats and labelled with chlorin  $e_6$  and was shown not to be toxic to MUC1<sup>-</sup> and MUC1<sup>+</sup> cells.

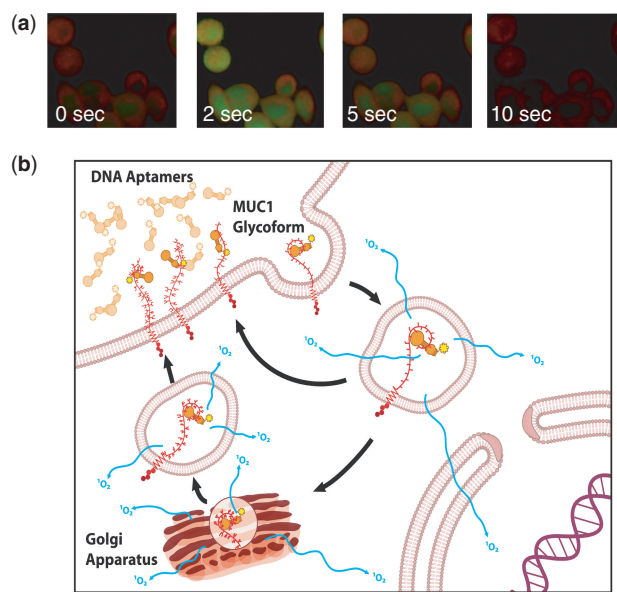


**Figure 6.** (a) Light activation of chlorin  $e_6$ -labelled aptamer 5TRG2 internalized by T47D cells produces toxic oxygen species observed across all cellular compartments. Visualization by two-photon confocal microscopy imaging of ROS production in T47D cells treated with Ce6-5TRG2 and the 5-(and-6-)-chloromethyl-2',7'-dichlorodihydrofluorescein diacetate acetyl ester (CM-H<sub>2</sub>DCFDA) as demonstrated by the appearance and fading of yellow colour over a 10 s photoradiation interval. (b) Proposed mechanism of action of phototoxic DNA aptamers directed at MUC1<sup>+</sup> epithelial cancer cell markers. Aptamers (orange) bind to membrane-bound, underglycosylated MUC1 mucin (red branched structures). These mucin structures are recycled from the cell surface to the Golgi network where they are further glycosylated before returning to the cell surface. PDT drugs coupled to such aptamers and relocated into epithelial cancer cells are activated by light to produce toxic  $^1\text{O}_2$  species resulting in selective cell death.

peptide or its related Tn antigens were armed to carry a cytotoxic cargo such as the light-activated PDT drug, chlorin  $e_6$ , their ability to kill epithelial cells was enhanced by several orders of magnitude upon light exposure in comparison to the free drug alone (Figure 5). This phenomenon was demonstrated for eight human MUC1<sup>+</sup> cancer cell lines (T47D, MCF-7, PANC-1, BxPC3, A549, MGH13, OVCAR-3, HT-29) representing five classes of epithelial cancer cells (breast, pancreas, lung, ovaries, colon). More importantly, the inability of anionic oligonucleotides to spontaneously enter cells resulted in no observable non-specific toxicity towards MUC1<sup>-</sup> cells (CHO, U87MG) or even to MUC1<sup>+</sup> normal human primary mammary epithelial cells displaying fully glycosylated MUC1 mucins (Figure 5). Our findings suggest that known cytotoxic drugs, prodrugs as well as oligonucleotide-based cargoes such as siRNAs, PNAs, ribozymes or antisense oligonucleotides could be coupled to deglycosylated mucin- and Tn antigen-directed aptamers in order to target and deliver them to a broad range of epithelial cancers. The recent design of chimeras involving RNA aptamers against the prostate-specific membrane antigen (PSMA) linked to siRNAs, supports our claim that aptamers can be used as directed delivery agents (5). However, siRNAs do require a very precise delivery since they are known to non-specifically activate

toll-like receptors leading to interferon production (26,27). In addition and as in the case of other cytotoxic agents, siRNAs may potentially kill non-targeted cell types if their cellular action triggers apoptotic mechanisms, a challenge that further emphasize the need for a focused delivery strategy. For this reason, we have employed a prodrug strategy illustrated in Figure 6b, where the PDT agent chlorin  $e_6$  is coupled to DNA aptamers, delivered into targeted cancer cells and activated by light to generate damaging singlet oxygen species and cell death.

Mechanistically, DNA aptamers directed at the MUC1 tandem repeat or its Tn antigen were rapidly internalized by receptor-mediated endocytosis (Figures 2 and 3), a result that correlates with Hughey and her coworkers (28,29) who showed that underglycosylated MUC1 mucins are recycled by clathrin-mediated endocytosis and trafficked through vesicular compartments including lysosomes. Our data suggest that such aptamers are routed through endosomal, lysosomal and Golgi compartments (Figures 2 and 4) but not to the nucleus of cells (Figure 4). Singlet oxygen species however do diffuse to all cellular locations (Figure 6a) implying that aptamer delivery to the nucleus or cytosol is not a necessary prerequisite for efficient toxicity to occur. One requirement may thus be that the toxic agent (either singlet oxygen, radiation or a diffusible drug) be able to relocate across cellular compartments.

Monoclonal antibodies to the extracellular portion of the MUC1 peptide domain and its Tn antigen are currently being evaluated as potential imaging and therapeutic agents (30,31). However, aptamers represent smaller, simpler, non-antigenic alternatives to antibodies and as presented in this study, display remarkably high specificity and affinity ( $K_d$ 's in the nanomolar range) for unique GalNAc-peptide structures specifically found on epithelial cancer cells. These findings suggest that the bivalent or multivalent nature of antibodies and lectins typically needed to recognize carbohydrate determinants are not required for DNA aptamers targeting GalNAc-containing mucin markers (Table 2). In addition, methods to chemically stabilize and alter the pharmacokinetics of aptamers have already led to the FDA approval of Macugen, a pegylated RNA aptamer directed at the vascular endothelial growth factor (VEGF) therapy and shown to help reduce the risk of vision loss in patients with neovascular age-related macular degeneration (32).

Finally, PDT is a safe, non-radioactive treatment modality that is well suited to treating a broad range of topical and luminal tissues using endoscopic light sources (via interstitial, bronchoscopic, colonoscopic or intraperitoneal procedures). Applications of PDT for treating patients with breast (33), prostate (34), lung (35) and oesophageal (36,37) cancers are now well documented. Nevertheless, there is a strong need to specifically deliver sensitizers to diseased cells in order to minimize damage caused to healthy tissues upon illumination (38). The phototoxic aptamers described in this study would directly address the issue of PDT toxicity to normal tissues since malignant cells derived from such tissues typically express unique mucin and Tn antigen surface signatures,

and would thus represent the only target of such PDT aptamers.

In summary, highly expressed and aberrantly glycosylated MUC1 determinants are found in greater than 90% of all primary and metastatic breast cancers (7,13) as well as most epithelial carcinomas (7). This study highlights that targeting small phototoxic DNA aptamers to underglycosylated determinants of MUC1 offers great potential in directing therapeutic agents to and into a broad range of epithelial cancer cells.

## SUPPLEMENTARY DATA

Supplementary Data are available at NAR Online.

## FUNDING

This study has been supported by a grant from the Canadian Breast Cancer Research Alliance in association with the Canadian Cancer Society (to J.G.). Funding for open access charge: Canadian Breast Cancer Research Alliance in association with the Canadian Cancer Society (to J.G.).

*Conflict of interest statement.* None declared.

## REFERENCES

- Feigon, J., Dieckmann, T. and Smith, F.W. (1996) Aptamer structures from A to [zeta]. *Chem. Biol.*, **3**, 611–617.
- Breaker, R.R. (1997) DNA aptamers and DNA enzymes. *Curr. Opin. Chem. Biol.*, **1**, 26–31.
- Ellington, A.D. and Szostak, J.W. (1990) In vitro selection of RNA molecules that bind specific ligands. *Nature*, **346**, 818–822.
- Tuerk, C. and Gold, L. (1990) Systematic evolution of ligands by exponential enrichment: RNA ligands to bacteriophage T4 DNA polymerase. *Science*, **249**, 505–510.
- McNamara, J.O. 2nd, Andrechek, E.R., Wang, Y., Viles, K.D., Rempel, R.E., Gilboa, E., Sullenger, B.A. and Giangrande, P.H. (2006) Cell type-specific delivery of siRNAs with aptamer-siRNA chimeras. *Nat. Biotechnol.*, **24**, 1005–1015.
- Brayman, M., Thathiah, A. and Carson, D.D. (2004) MUC1: a multifunctional cell surface component of reproductive tissue epithelia. *Reprod. Biol. Endocrinol.*, **2**, 4.
- Gandler, S.J. (2001) MUC1, the renaissance molecule. *J. Mammary Gland Biol. Neoplasia*, **6**, 339–353.
- Litvinov, S.V. and Hilken, J. (1993) The epithelial sialomucin, episialin, is sialylated during recycling. *J. Biol. Chem.*, **268**, 21364–21371.
- Ceriani, R.L., Chan, C.M., Baratta, F.S., Ozzello, L., DeRosa, C.M. and Habif, D.V. (1992) Levels of expression of breast epithelial mucin detected by monoclonal antibody BrE-3 in breast-cancer prognosis. *Int. J. Cancer*, **51**, 343–354.
- Altschuler, Y., Kinlough, C.L., Poland, P.A., Bruns, J.B., Apodaca, G., Weisz, O. A. and Hughey, R.P. (2000) Clathrin-mediated Endocytosis of MUC1 is modulated by its glycosylation state. *Mol. Biol. Cell*, **11**, 819–831.
- Henderikx, P., Coolen-van Neer, N., Jacobs, A., van der Linden, E., Arends, J.W., Müllberg, J. and Hoogenboom, H.R. (2002) A human immunoglobulin G1 antibody originating from an in vitro-selected Fab phage antibody binds avidly to tumor-associated MUC1 and is efficiently internalized. *Am. J. Pathol.*, **160**, 1597–1608.
- Burchell, J.M., Mungul, A. and Taylor-Papadimitriou, J. (2001) O-linked glycosylation in the mammary gland: changes that occur during malignancy. *J. Mammary Gland Biol. Neoplasia*, **6**, 355–364.
- Cheung, K.L., Graves, C.R. and Robertson, J.F. (2000) Tumour marker measurements in the diagnosis and monitoring of breast cancer. *Cancer Treat. Rev.*, **26**, 91–102.
- Ho, J.J. (2000) Mucins in the diagnosis and therapy of pancreatic cancer. *Curr. Pharm. Des.*, **6**, 1881–1896.
- Price, M.R., Rye, P.D., Petrakou, E., Murray, A., Brady, K., Imai, S., Haga, S., Kiyozuka, Y., Scho, I. D., Meulenbroek, M.F. et al. (1999) Mimics and cross reactions of relevance to tumour immunotherapy. *Vaccine*, **18**, 268–275.
- Price, M.R., Rye, P.D., Petrakou, E., Murray, A., Brady, K., Imai, S., Haga, S., Kiyozuka, Y., Scho, I. D., Meulenbroek, M.F. et al. (1998) Summary report on the ISOBM TD-4 Workshop: analysis of 56 monoclonal antibodies against the MUC1 mucin. San Diego, Calif., November 17–23, 1996. *Tumour Biol.*, **19** (Suppl. 1), 1–152.
- Brokx, R.D., Revers, L., Zhang, Q., Yang, S., Mal, T.K., Ikura, M. and Gariépy, J. (2003) Nuclear magnetic resonance-based dissection of a glycosyltransferase specificity for the mucin MUC1 tandem repeat. *Biochemistry*, **42**, 13817–13825.
- Ferreira, C.S.M., Matthews, C.S. and Missailidis, S. (2006) DNA aptamers that bind to MUC1 tumour marker: design and characterization of MUC1-binding single-stranded DNA aptamers. *Tumour Biol.*, **27**, 289–301.
- McCabe, P.C. (1990) Production of single-stranded DNA by asymmetric PCR. In Innis, M.A., Gelfand, D.H., Sninsky, J.J. and White, T.J. (eds), *PCR Protocols*, Academic Press, San Diego, pp. 76–83.
- Linsley, P.S., Brown, J.P., Magnani, J.L. and Horn, D. (1988) Monoclonal antibodies reactive with mucin glycoproteins found in sera from breast cancer patients. *Cancer Res.*, **48**, 2138–2148.
- Plumb, J.A. (2004) Cell sensitivity assays: the MTT assay. *Methods Mol. Med.*, **88**, 165–169.
- Calafat, J., Molthoff, C., Janssen, H. and Hilken, J. (1988) Endocytosis and intracellular routing of an antibody-ricin A chain conjugate. *Cancer Res.*, **48**, 3822–3827.
- Bradley, J.R., Johnson, D.R. and Pober, J.S. (1993) Four different classes of inhibitors of receptor-mediated endocytosis decrease tumour necrosis factor-induced gene expression in human endothelial cell. *J. Immunol.*, **150**, 5544–5555.
- Ray, E. and Samanta, A.K. (1997) Dansyl cadaverine regulates ligand induced endocytosis of interleukin-8 receptor in human polymorphonuclear neutrophils. *FEBS Lett.*, **378**, 235–239.
- Chow, J.C., Condorelli, G. and Smith, R.J. (1998) Insulin-like growth factor-I receptor internalization regulates signaling via the Shc/mitogen-activated protein kinase pathway, but not the insulin receptor substrate-1 pathway. *J. Biol. Chem.*, **273**, 4672–4680.
- Kariko, K., Bhuyan, P., Capodici, J. and Weissman, D. (2004) Small interfering RNAs mediate sequence-independent gene suppression and induce immune activation by signalling through toll-like receptor 3. *J. Immunol.*, **172**, 6545–6549.
- Sledz, C.A., Holko, M., Veer, M.J., Silverman, R.H. and Williams, B.R. (2003) Activation of the interferon system by short-interfering RNAs. *Nat. Cell Biol.*, **5**, 834–839.
- Altschuler, Y., Kinlough, C.L., Poland, P.A., Bruns, J.B., Apodaca, G., Weisz, O.A. and Hughey, R.P. (2000) Clathrin-mediated endocytosis of MUC1 is modulated by its glycosylation state. *Mol. Biol. Cell*, **11**, 819–831.
- Kinlough, C.L., Poland, P.A., Bruns, J.B., Harkleroad, K.L. and Hughey, R.P. (2004) MUC1 membrane trafficking is modulated by multiple interactions. *J. Biol. Chem.*, **279**, 53071–53077.
- Salouti, M., Rajabi, H., Babaei, M.H. and Rasaei, M.J. (2008) Breast tumor targeting with (99m)Tc-HYNIC-PR81 complex as a new biologic radiopharmaceutical. *Nucl. Med. Biol.*, **35**, 763–768.
- Manimala, J.C., Li, Z., Jain, A., VedBrat, S. and Gildersleeve, J.C. (2005) Carbohydrate array analysis of anti-Tn antibodies and lectins reveals unexpected specificities: implications for diagnostic and vaccine development. *Chembiochem*, **6**, 2229–2241.
- Gragoudas, E.S., Adamis, A.P., Cunningham, E.T., Feinsod, M. and Guyer, D.R. (2004) Pegaptanib for neovascular age-related macular degeneration. *New Engl. J. Med.*, **351**, 2805–2816.

33. Cuenca,R.E., Allison,R.R., Sibata,C. and Downie,G.H. (2004) Breast cancer with chest wall progression: treatment with photodynamic therapy. *Ann. Surg. Oncol.*, **11**, 322–327.
34. Du,K.L. *et al.* (2006) Preliminary results of interstitial motexafin lutetium-mediated PDT for prostate cancer. *Lasers Surg. Med.*, **38**, 427–434.
35. Moghissi,K., Dixon,K., Thorpe,J.A., Stringer,M. and Oxtoby,C. (2007) Photodynamic therapy (PDT) in early central lung cancer: a treatment option for patients ineligible for surgical resection. *Thorax*, **62**, 391–395.
36. Acroyd,R. *et al.* (2003) Eradication of dysplastic Barret's oesophagus using photodynamic therapy: long-term follow-up. *Endoscopy*, **35**, 496–501.
37. Moghissi,K., Dixon,K., Thorpe,J.A., Stringer,M. and Moore,P.J. (2000) The role of photodynamic therapy (PDT) in inoperable oesophageal cancer. *Eur. J. Cardiothorac Surg.*, **17**, 95–100.
38. Hahn,S.M. *et al.* (2006) Photofrin uptake in the tumour and normal tissues of patients receiving intraperitoneal photodynamic therapy. *Clin. Cancer Res.*, **12**, 5464–5470.